Geophys. J. Int. (2004) **159,** 679–687 doi: 10.1111/j.1365-246X.2004.02407.x

Probabilities of activation of seismic faults in critical regions of the Aegean area

C. B. Papazachos, G. F. Karakaisis, E. M. Scordilis and B. C. Papazachos

Geophysical Laboratory, University of Thessalonki 54124, *Greece. E-mails: costas@lemnos.geo.auth.gr (CBP); karakais@geo.auth.gr (GFK); manolis@geo.auth.gr (EMS); basil@lemnos.geo.auth.gr (BCP)*

Accepted 2004 June 16. Received 2003 November 11; in original form 2003 January 6

SUMMARY

Properties of the accelerating seismic crustal deformation pattern and of the intermediate-term seismic quiescence pattern have been combined to identify faults in the Aegean area (34°N–43°N, 19°E–30°E) that have a considerable probability of generating strong earthquakes ($M \geq 6.4$) during the next 5-yr period. Eight groups of such faults have been identified, and the probability of each fault being activated during this time period has been estimated. Three of these groups are located in southern Greece (Hellenic Arc), two in central Greece (East Central Greece, Ionian Islands), two in northwestern Turkey and one in the area of the borders of Albania, Greece and the Former Yugoslav Republic of Macedonia. The importance of these results for intermediate-term seismic hazard assessment is discussed.

Key words: accelerating seismic deformation, Aegean area, critical regions, seismic faults, seismic quiescence.

INTRODUCTION

Recent research work on precursory seismic patterns indicates that there are two different patterns, the investigation of which appears to be promising for intermediate-term prediction of strong earthquakes. The first of these patterns concerns accelerating seismic energy release by the generation of intermediate-magnitude pre-shocks, which is related to critical point dynamics (Sornette & Sornette 1990; Sornette & Sammis 1995; Jaume & Sykes 1999). The second pattern concerns seismicity quiescence (decrease in the rate of shocks) in the rupture zone of a future main shock, probably related to dilatancy hardening or slip weakening (Wyss & Habermann 1988; Scholz 1988; Wyss 1997; Zoller *et al.* 2002). Although the two patterns seem to be in opposition, since the one shows an increase in seismicity (seismic excitation) and the other a decrease in seismicity (seismic quiescence) before a main shock, in reality they are not because, as we are going to show, they occur in different spaces and at different seismic energy levels. It appears that the two patterns have properties such that the corresponding two techniques, which are based on these patterns, can be applied in a complementary way to improve our approach to intermediate-term earthquake prediction. For this reason it is of interest to describe briefly the basic properties of these two patterns.

The pre-shocks, the generation of which causes the accelerating deformation pattern, are of intermediate magnitude (e.g. for main shocks larger than 6.5 pre-shocks are larger than 4.8; Bufe & Varnes 1993; Papazachos 2003). It is the increase in the number of pre-shocks as well as in their magnitudes which contributes to the acceleration of seismic crustal deformation (Benioff strain) with time to the main shock (eq. 1). The region where the foci of the pre-shocks are located (critical region) scales with the magnitude of the main shock (Bowman *et al.* 1998) and its dimension is about eight times larger than the fault length of the corresponding main shock (Papazachos & Papazachos 2000). The duration of the pre-shock sequence decreases with increasing mean seismicity rate for the region (Papazachos & Papazachos 2001), as also occurs for the time interval, $\Delta t_i = t_c - t_i$, between the origin time, t_c, of the main shock and the time, t_i, when accelerating deformation started to be identifiable (Papazachos & Papazachos 2001; Yang *et al.* 2001). This time interval, Δt_i, when intense release of seismic energy takes place in critical regions of the Aegean area, is, on average, equal to 3.7 ± 1.6 yr (Papazachos *et al.* 2003b).

A decrease in the rate of the relatively small pre-shocks is a basic property of an intermediate-term seismic quiescence pattern. Such a decrease of seismicity takes place in the fault region and usually covers the whole after-shock region (Wyss *et al.* 1981; Wyss 1986). The duration of pre-shock quiescence seems to scale with magnitude (Mogi 1981) but the considerable scatter of the data does not permit a reliable estimation of the magnitude of the ensuing main shock from this duration. Such approximate relations (Scholz 1988) suggest that the quiescence period has duration of about 4 yr for earthquakes with magnitude 7.0, that is, about equal to the duration of the intense seismic excitation in the broader critical region. Therefore, it appears that the two precursory phenomena take place at about the same time interval but for different spatial extents and levels of seismic energy. This behaviour is similar to a 'doughnut pattern', i.e. quiescence in the source region of a future main shock and excitation in the broader surrounding region (Mogi 1981). Hence, it can be suggested that intermediate-term earthquake prediction based on the accelerating deformation method may be considerably

improved if properties of the intermediate-term seismic quiescence pattern are also taken into account. This improvement should be particularly applicable for a more precise location of the ensuing main shock, since the quiescence patterns occur in the main-shock fault area. A further improvement in this location can be made if the seismic faults located in the pre-shock (critical) region of this main shock are known.

The main goal of the present study is to use properties of both these patterns to identify faults in Greece and the surrounding area where probabilities for the occurrence of strong main shocks ($M \geq 6.4$) during the next 5 yr or so are high and to estimate the probability of rupture for each of these faults.

DATA AND IDENTIFICATION OF CRITICAL REGIONS

The data used in the present study come from the catalogue of Papazachos *et al.* (2003a), which for Greece and the surrounding area (34°N–43°N, 19°E–30°E) includes historical data since the fifth century BC and instrumental data from 1911, when the first seismograph (Mainka type) was installed in Athens, until 2002 September 30. All magnitudes in this catalogue are equivalent moment magnitudes, M, and the instrumental data are complete for the following periods and corresponding magnitudes:

1911–2002, $M \geq 5.2$
1950–2002, $M \geq 5.0$
1965–2002, $M \geq 4.5$
1981–2002, $M \geq 4.0$.

The improvement in completeness in 1950 is due to the organization of a dense macroseismic observation network, while the change in 1965 reflects the installation of the first seismographic network in Greece by the Geodynamic Institute of the National Observatory of Athens. Finally, the 1981 change corresponds to the installation of the first telemetric network of stations by the Geophysical Laboratory of the University of Thessaloniki. The errors in the magnitudes are less than 0.3, while the errors in the epicentres are less than 35, 30, 20 and 15 km since 1911, 1950, 1965 and 1981, respectively. Due to improvement in the velocity models used, the uncertainties in the epicentre locations have been significantly improved since 1985. Data for shallow earthquakes ($h \leq 40$ km) were used for the whole area, except for the Hellenic Arc (South Greece) where data for shallow and intermediate-depth shocks ($h \leq 100$ km) were incorporated.

Identification of an elliptical geographical region which is in a state of accelerating seismicity (critical region) was made by the 'method of accelerating seismic crustal deformation' (Papazachos & Papazachos 2001), which is a step-wise procedure based on several properties of the time-to-failure model. The accelerated seismicity (deformation) model is typically expressed with the following power-law relation:

$$S = A + B(t_c - t)^m \tag{1}$$

which relates the cumulative Benioff strain, S (square root of the seismic energy), released by the intermediate-magnitude shocks (pre-shocks), with the origin time, t_c, of the main shock (Bufe & Varnes 1993). In eq. (1) t_c is the main-shock time and A, B and m are parameters. The Benioff strain, S, is calculated from the moment magnitudes of the earthquakes, using appropriate relations.

In practice the model is applied to real earthquake data by minimizing a curvature parameter, C, which quantifies the degree of deviation of the Benioff strain from linearity (acceleration). This parameter was defined as the ratio of the root-mean square error of the power-law fit (eq. 1) to the corresponding linear fit error and has been proposed by Bowman *et al.* (1998) for the identification of circular regions approaching criticality, mainly along the San Andreas fault system since 1950. The same authors showed that the logarithm of the radius of the pre-shock area scales with the expected main-shock magnitude. Papazachos & Papazachos (2000, 2001) extended this approach to elliptically shaped areas and proposed four additional semi-empirical relations, which can be used as constraints for applications using real data. To quantify the compatibility of these relations with observations an appropriate parameter P was defined (Papazachos & Papazachos 2001), which quantifies the compatibility of an observed accelerated deformation pattern with previous similar observations. Furthermore, Papazachos *et al.* (2002a) have proposed a quality measure, q, defined by the relation:

$$q = \frac{P}{mC} \tag{2}$$

in an attempt to simultaneously evaluate several aspects of an observed accelerated deformation pattern, namely:

(1) The compatibility of an accelerating seismic deformation with the behaviour of past real accelerated deformation pre-shock sequences (large values of P).
(2) The deviation of the variation with time of the seismic deformation from linearity (small values of C) as proposed by Bowman *et al.* (1998).
(3) The degree of seismic acceleration (small m values).

Investigation of pre-shock sequences of strong main shocks ($M \geq 6.4$) which have occurred in the Aegean since 1950 has led to the adoption of the following cut-off values:

$$C \leq 0.6, \quad m \leq 0.35, \quad P \geq 0.45, \quad q \geq 3.0 \tag{3}$$

with typical average values $[C] = 0.44$, $[m] = 0.29$, $[P] = 0.53$ and $[q] = 4.9$.

Application of this method to several pre-shock sequences in Greece and other areas has shown that the seismic excitation in an elliptical critical region centred at a certain point depends not only on q but also on other measurable quantities such as the magnitude M of the expected main shock, the number, N, of valid solutions (solutions at each geographical point which fulfil eq. 3) with different elliptical regions centred at the same point and the percentage, λ, of the neighbouring points of the grid for which valid solutions exist. Thus, a quantity, K, called the excitation indicator, is defined by the relation:

$$K = q\frac{M}{M_c}\sqrt{\frac{N}{N_c}}\lambda. \tag{4}$$

It is clear that K attempts to modify q in order to further focus on larger main shocks (large M values) and areas with a large number of solutions (high N values) and a high number of solutions in neighbouring areas (high λ values), in accordance with Yang *et al.* (2001) who present evidence that *a posteriori* predictions for past main shocks show that they occur in the vicinity of those areas with a higher density of obtained accelerated deformation solutions. M_c and N_c are used in order to return K values which are of a similar order of magnitude to the original definition of q by Papazachos *et al.* (2002a). However, since results obtained for past earthquakes in the Aegean area show that K varies between different areas, a normalized value, K_n, is defined for each geographical point, which

is the ratio of the value of K calculated for this point to its maximum value observed for any pre-shock sequence in that area. K_n varies between 0 and 1, while M_c is a constant magnitude (e.g. $M = 7.0$) and N_c is a constant number (e.g. $N_c = 10$).

Unfortunately, accelerated deformation patterns which fulfil the criteria of eq. (3) are only observed a few months to a couple of years before the expected main shock. Accelerating seismic deformation behaviour that fulfils 'looser' criteria ($m \leq 0.7$, $C \leq 0.7$) can also be identified at a time, t_i, before the occurrence of the main shock, which can be described as the identification time, t_i, for this phenomenon. It has been shown (Papazachos & Papazachos 2001) that the difference, $t_c - t_i$, between the identification time and the origin time, t_c, of the main shock is given by the relation:

$$\log(t_c - t_i) = 5.04 - 0.75 \log s_r \quad (5)$$

where s_r (in $J^{1/2}$ yr^{-1} 10^{-4} km^{-2}) is the long-term Benioff strain rate per unit area. Hence, the identification period decreases with increasing seismicity of the pre-shock (critical) region, as also occurs for the total duration, t_p, of the pre-shock period. The identification period, $t_c - t_i$, is about 17 per cent of the duration, t_p, of the corresponding pre-shock period, in accordance with independent estimates (Yang *et al.* 2001).

An appropriate algorithm has been developed (Papazachos 2001) to apply the previous results to the identification of a pre-shock (critical) region. According to this algorithm, shocks (pre-shocks) with epicentres in an elliptical region centred at a certain geographical point (assumed epicentre of the main shock) are considered and parameters of eq. (1), as well as the curvature parameter, C, are calculated. Calculations are repeated by applying a systematic search of a large set of values for the azimuth, z, of the large ellipse axis, its length, a, ellipticity, e, and the time, t_s, since accelerating seismic deformation started, for the magnitude, M, and the origin time, t_c, of the main shock. These computations are repeated for a grid of points in which the investigated area is separated by the desired density (e.g. 0.2°NS, 0.2°EW). The geographical point which corresponds to the best solution (largest value of K) is considered as a first approximation of the epicentre of the expected main shock, and the magnitude which corresponds to this solution is considered as the magnitude of the main shock. The epicentre which is finally adopted is also based on additional information, such as the location of seismic faults in the region.

Application of this method to real data usually results in a large number of solutions and large errors, especially for the origin time, t_c, due to the trade-offs between the model parameters of eq. (1). For this reason the mean value of $m(= 0.29)$ observed for real data was adopted in all calculations, similar to numerous other studies (e.g. Zoller & Hainzl 2002), in excellent agreement with theoretical considerations which report m values ranging from 0.25 to 0.33 (Ben-Zion *et al.* 1999; Rundle *et al.* 2000). Furthermore, the origin time of the oncoming main shock is calculated not only by direct application of eq. (1) with a constant value of $m(= 0.29)$, but also by the application of eq. (5) and an additional approach proposed by Papazachos *et al.* (2001a), which relies on the observation of pre-shock excitation that occurs close to the identification time, t_i, and permits the simultaneous calculation of t_i and t_c. It should be noted that the estimation of t_c from t_i is performed for the critical area identified using the 'loose' criteria, which are used for the determination of the identification time, t_i. However, we should point out that in all cases examined *a posteriori* for the Aegean area (Papazachos & Papazachos 2000, 2001) critical regions show a remarkable stability of their spatial dimensions, whether they are determined using the 'loose' or strict criteria presented by eqs (3).

The previously described procedure has been used to identify elliptical regions which are currently in a state of accelerating seismicity in the broader Aegean area (34°N–43°N, 19°E–30°E) by using data (epicentres, origin times, magnitudes of shocks with $M \geq 4.5$) for earthquakes which occurred up to 2002 September 30. Eight such regions have been identified. Five of these regions have centres in Greece (1, southwestern Hellenic Arc; 2, East Central Greece; 3, Ionian Sea; 4, East Hellenic Arc; 5, southeast Aegean, in Table 1), and one in the borders between Albania, the Former Yugoslav Republic of Macedonia and Greece (6, South Albanides, in Table 1) and two in northwestern Turkey (7, southwest of Marmara; 8, southeast of Marmara, in Table 1). In Fig. 1 the centres of these eight regions are denoted by stars. Furthermore, the elliptical critical areas and the corresponding pre-shocks are also presented. The corresponding Benioff-strain acceleration patterns are presented in Fig. 2. The number of each centre corresponds to the number in Table 1 where information is given about the parameters of the probable expected main shocks and of the assumed pre-shock sequence. As can be concluded from the values of the origin times, t_c, taking into consideration their uncertainties (±2.0 yr), these 'predicted' main shocks are expected to occur during the years 2003–2007. Magnitudes of the expected main shocks vary between 6.4 and 7.0 and the optimal magnitude difference between the main shock and smallest pre-shock for this magnitude is 1.7–1.9 (Papazachos 2003), while the duration of the pre-shock sequences varies between 10 and 35 yr (Papazachos & Papazachos 2000; 2001).

Except for the critical regions in Central Greece and the Ionian Islands (numbers 2 and 3 in Table 1) information for all other regions has been previously derived on the basis of the available data, which concern earlier stages of accelerating deformation (Papazachos

Table 1. Information on the eight critical regions, which are currently in a state of accelerating seismic deformation. The first three columns give the code number, the name of the region and the geographical coordinates, Φ, Λ of the centres of the eight elliptical regions. M is the estimated magnitude of the expected main shock and t_c is its estimated time of origin. a (in km) is the length of the large axis of the ellipse with ellipticity e and z is its azimuth. M_{min} is the minimum magnitude of shocks (pre-shocks), n their number and t_s the start year of the pre-shock sequence. q is the quality factor and K is the excitation indicator.

No	Region	Φ, Λ	M	t_c	a	z	e	M_{min}	n	t_s	q	K
1	SW Hellenic Arc	36.4, 23.2	6.9	2006.4	310	60	0.95	5.1	37	1959	7.4	16.5
2	E Central Greece	38.8, 23.4	6.8	2004.8	236	0	0.90	5.1	21	1984	9.1	7.2
3	Ionian Islands	38.2, 20.9	7.0	2005.2	312	90	0.95	5.3	28	1984	3.1	0.6
4	E Hellenic Arc	35.0, 28.3	6.7	2006.6	200	120	0.90	5.0	34	1980	6.7	5.9
5	SE Aegean	37.4, 26.7	6.8	2005.6	190	30	0.80	5.1	22	1975	4.5	2.6
6	S Albanides	41.0, 21.2	6.7	2005.2	200	60	0.90	5.0	26	1975	3.9	2.0
7	SW Marmara	40.2, 27.2	6.4	2004.1	161	0	0.90	4.7	29	1984	7.5	8.4
8	SE Marmara	39.4, 29.2	6.9	2004.9	192	150	0.70	5.0	50	1974	7.4	12.4

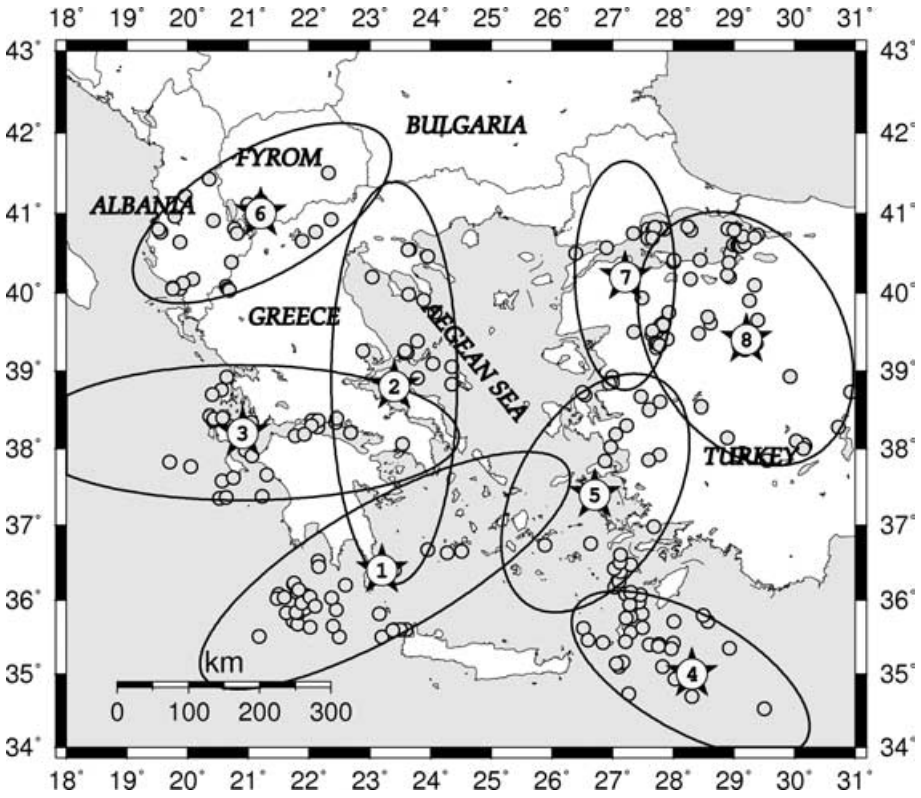

Figure 1. Centres of the eight elliptical critical regions in Greece and the surrounding area, which currently exhibit an accelerating seismic excitation. The elliptical critical regions, as well as the corresponding intermediate-magnitude events (pre-shocks) are also shown. The numbers correspond to the code numbers in Table 1. FYROM = Former Yugoslav Republic of Macedonia.

et al. 2002a,b,c). A very good agreement of the new solutions with older ones is observed with respect to the magnitudes and the locations of the centres of the critical regions; however, the estimated origin times differ. This bias is obviously due to the fact that the estimation of the origin time is sensitive to the behaviour of the last phase of the accelerating seismic deformation and to the recent improvement of the method (introduction of the excitation parameter K, use of a constant value of m, etc.). This observation suggests that real uncertainties in the estimation of the origin time, t_c, are perhaps higher than previously estimated ($\pm$2.0 yr, Papazachos *et al.* 2001a). For this reason, continuous monitoring and recalculation of parameters of the identified pre-shock regions is necessary.

ASSOCIATION OF CRITICAL REGIONS WITH ACTIVE FAULTS AND QUIESCENCE PATTERNS

The next step in the present work was to identify the major faults located in a broad area around the centre of each critical region ($\sim$120 km) and re-examine the parameters of the intermediate-magnitude earthquakes, which are located in a broad region that 'engulfs' each fault. Parameters for the main active seismic faults were taken from Papazachos *et al.* (2001b), which includes information for 164 faults (160 shallow and four of intermediate depth), which are probably associated with all known strong events in the broader Aegean area. Of the seismic faults for which information is presented by Papazachos *et al.* (2001b), about 120 faults are large, i.e. have fault lengths equal to or larger than 30 km. About 35 per cent of these large faults are located within the eight critical regions which have been identified by the procedure described in the previous section, that is, about five such faults are included in each critical region. From all faults in each critical region we selected three faults for further investigation, on the basis of their sizes (the larger ones), their long-term activity (the most active ones) and of the current intermediate-magnitude activity in the broader region, which surrounds each fault (Fig. 1). All these faults are presented in Fig. 3 and are all shallow except for fault 1.3, which is of intermediate focal depth. Thirteen of these faults are normal, seven are strike-slip and four are thrust faults.

We should point out that in the present work we have selected to proceed from a grid search of accelerated deformation in the broader Aegean area to the selection of the main faults which are located close to the vicinity of the centre of these critical regions. Alternatively, we could start from the 120 most important faults and examine the presence of accelerated deformation considering their centre as the centre of the critical region. The only reason that the former approach was adopted was that we wanted to examine the possibility of identification of accelerated deformation in regions where no major faults have yet been identified, such as regions in the Aegean Sea where no surface manifestation of active faults can be identified and active faults are mainly determined on the basis of seismic activity.

In order to further constrain the possibility of seismic activation in the faults of each critical area we have examined the existence of intermediate-term quiescence in the vicinity of each of the three faults of a critical region. Since a relatively accurate data sample is necessary for this step, shocks with $M \geq 4.0$ which have occurred since 1985 were used, using a minimum data sample of 31 shocks. For each of these faults, which are possibly at quiescence now, an

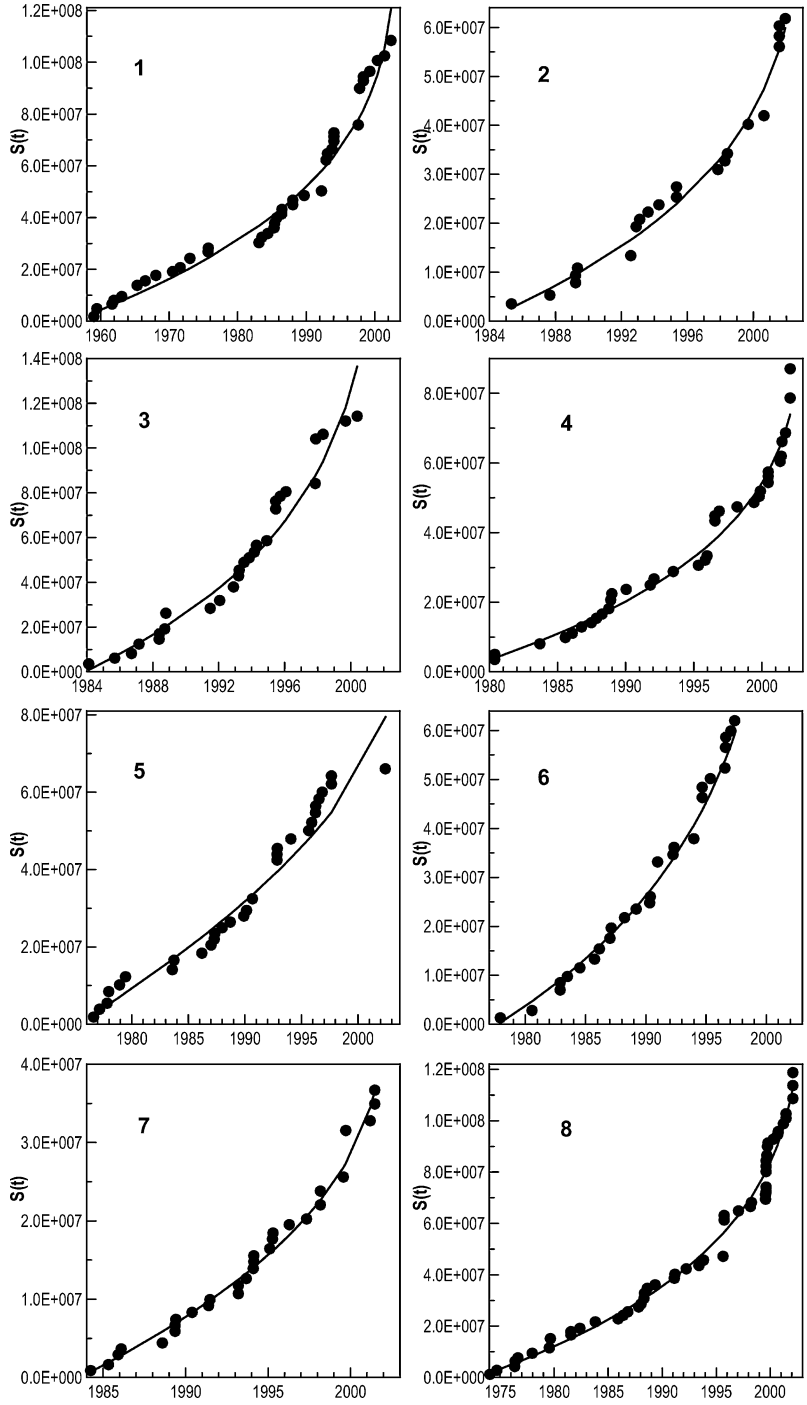

Figure 2. Accelerated variation of the Benioff strain with time for the eight critical regions presented in Fig. 1.

elliptical region (with ellipticity 0.70) centred at the middle of the fault and having its large axis parallel to the fault was considered. The size of the examined region around each fault was allowed to vary from ∼80 per cent of the fault length up to 1.5 fault lengths, while the centre of the search area was also allowed to move up to 25 per cent of the fault length along the fault strike and 10 per cent of the fault length normal to its strike, in an attempt to account for errors in the location of shocks with $M \geq 4.0$ associated with this event, keeping the minimum number of events greater than 30 for the period 1985–2002.

Examination of the cumulative number of these shocks as a function of time allowed the identification of clear quiescence patterns, usually for one of the three faults within each critical region. The start of the quiescence period was also allowed to vary. On the basis of these observations, several parameters were determined, namely the quiescence area (gap of the second kind), the start time, T_s, of the quiescence period, the annual rate, r, of shocks during the quiescence period, the annual rate, r_m, of shocks between 1985 and the start of quiescence period (background seismicity), and their ratio, $r_n = r/r_m$, which was considered as an indicator of the degree of quiescence. The results show that the length of the identified quiescence area varies between one fault length and two and half fault lengths, with an average about two fault lengths (1.9 ± 0.4), while the quiescence durations (up to the end of the catalogue used) vary

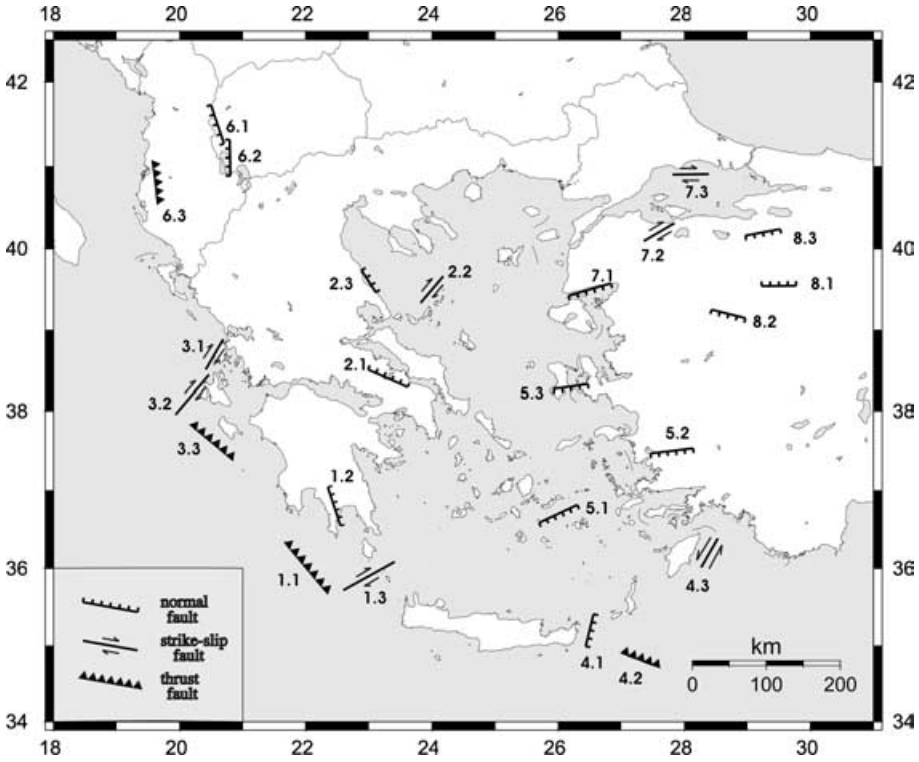

Figure 3. The eight groups of seismic faults located in the corresponding critical regions, which were examined for quiescence patterns. Numbers correspond to code numbers in Table 2.

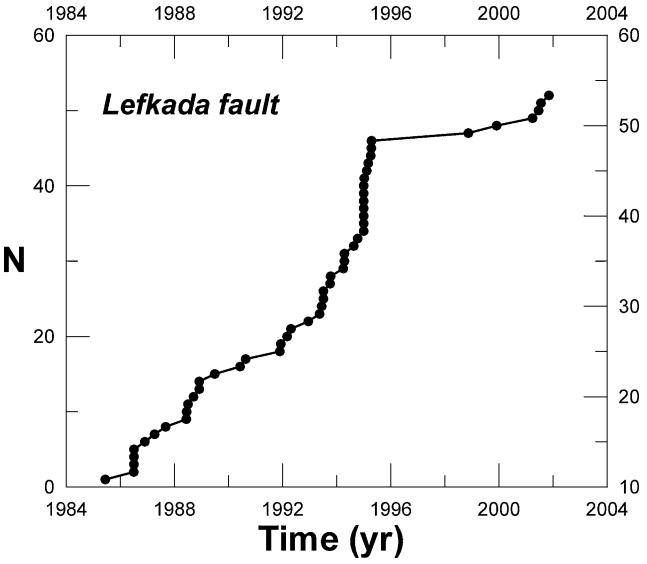

Figure 4. Variation of the number of earthquakes, N, as a function of time for the Lefkada Fault (3.1 in Fig. 3), using the procedure described in the present work. A clear quiescence pattern is observed after 1995.

between 3 and 7 yr, with an average 4.5 yr (4.5 $\pm$ 1.6 yr). A typical quiescence pattern is presented for the Lefkada Fault, where seismic quiescence is clearly observed after 1995 (Fig. 4).

In order to quantify and combine results from critical area identification and seismic quiescence, an attempt to assess the probability, P_e, of the occurrence in each fault of the main shock expected in the corresponding critical region during the period 2003–2007 has been performed. The faults in a critical region, which is in an accelerated seismic excitation, all have some increased probability of being activated by triggering due to the accelerating generation of intermediate-magnitude shocks in this region. Those faults, which are located in a broader region with a high degree of seismic crustal deformation (high value of K_n) and are included in a narrower region of decreased seismicity (low value of r_n) should have the highest probability of activation. Therefore it is reasonable to assume that the ratio, D_n, of K_n to r_n can be used as a preliminary but appropriate measure of the potential for the occurrence of a main shock in this fault. By summing all D_n values and dividing the D_n value for each fault by this sum we can assess a probability for the occurrence of the main shock in this fault, considering that the probability for the occurrence of the main shock in any fault of the critical region is equal to unity. If we assume a different value for this last probability, the obtained results (probabilities) must be multiplied by this total probability to get P_e for each fault. In the present work, we considered a total probability of 75 per cent, since there is a 10 per cent probability that the expected main shock occurs outside the confidence intervals defined by Papazachos *et al.* (2003b) and there is a 15 per cent probability that the observed accelerated patterns can be obtained from random catalogues, as shown from Monte Carlo tests (Papazachos *et al.* 2002a).

RESULTS

Table 2 gives information on the parameters of these 24 faults that are grouped in eight clusters (critical areas of Fig. 1). In the last column of Table 2 the year and the magnitude are given for the last damaging main shocks of each fault. The macroseismic effects of these main shocks are described in detail in Papazachos & Papazachou (2003). These data are important for intermediate-term seismic risk assessment because they can be reliably used for

Table 2. Information on the main seismic faults located in the eight critical regions investigated in the present study. Φ and Λ are the geographical coordinates of the fault centre, while L, ξ, θ and λ are the length (in km), strike, dip and rake of the fault, respectively. K is the excitation indicator in the broad critical region, r_n is the quiescence indicator in the vicinity of the fault, D_n is the activation potential and P_e is the probability of occurrence of a strong ($M \geq 6.4$) main shock during the 5 yr 2003–2007. The last column gives the year and the magnitude of the most damaging recent main shocks for each fault.

No	Name	ϕ°_N, Λ°_E	L	ξ	θ	λ	K	r_n	D_n	P_e	Year (M)
1. SW Hellenic Arc											
1.1	Tenaro	36.00, 22.00	70	320	32	106	18.4	1.19	15.46	0.32	1903 (7.2)
1.2	Sparti-Gythio	36.73, 22.53	60	346	47	−98	6.10	0.46	13.26	0.28	1867 (6.8), 1927 (7.1)
1.3	Cythera	35.90, 23.00	70	61	70	144	8.20	1.13	7.26	0.15	1910 (6.8), 1926 (7.2)
2. East Central Greece											
2.1	Atalanti	38.57, 23.25	50	294	50	−70	3.30	0.88	3.75	0.11	1894 (7.0)
2.2	N Sporades	39.42, 24.10	40	40	77	175	3.20	0.54	5.93	0.18	1965 (6.1)
2.3	Keramidi	39.58, 23.04	30	327	50	−70	1.50	0.10	15.00	0.46	1930 (6.1), 1955 (6.2)
3. Ionian Islands											
3.1	Leukada	38.70, 20.55	40	30	77	178	0.20	0.17	1.18	0.26	1914 (6.3), 1948 (6.5)
3.2	Cephalonia	38.20, 20.20	60	40	57	172	0.30	0.21	1.43	0.32	1953 (7.2), 1983 (7.0)
3.3	Zakynthos	37.58, 20.53	55	310	18	118	0.20	0.27	0.74	0.17	1953 (6.8), 1997 (6.6)
4. East Hellenic Arc											
4.1	Zakros(E Crete)	35.16, 26.49	40	14	47	−198	1.10	1.08	1.02	0.16	1922 (6.8)
4.2	Strabo Trench	34.80, 27.30	40	291	47	99	1.80	0.58	3.10	0.50	1948 (7.1)
4.3	Rhodes	36.25, 28.40	40	30	80	−41	0.20	0.37	0.54	0.09	1896 (6.4), 1957 (7.2)
5. SE Aegean											
5.1	Amorgos	36.73, 25.99	50	65	40	−90	1.82	0.86	2.12	0.59	1956 (7.5)
5.2	Aydin	37.87, 28.16	50	83	42	−99	0.69	2.11	0.33	0.09	1899 (7.0), 1955 (6.9)
5.3	South Chios	38.29, 26.20	40	82	45	−115	0.89	3.33	0.27	0.07	1881 (6.5), 1949 (6.7)
6. S. Albanides											
6.1	Peshkopi	41.46, 20.56	45	161	49	−87	1.30	0.58	2.24	0.13	1922 (6.1), 1967 (6.3)
6.2	Ochrid	41.02, 20.79	40	179	49	−87	2.00	0.29	6.90	0.39	1911 (6.7)
6.3	Fier	40.80, 19.56	40	353	27	93	2.00	0.50	4.00	0.23	185 (6.8), 1962 (6.0)
7. SW Marmara											
7.1	Edremit	39.49, 26.46	50	74	46	−114	2.42	0.95	2.24	0.14	1944 (6.9)
7.2	Sarikoy	40.24, 27.60	40	240	70	−155	3.63	0.43	6.90	0.46	1983 (6.4)
7.3	N Marmaras	40.90, 28.13	40	89	90	177	1.81	0.65	4.00	0.15	1648 (6.8)
8. SE Marmara											
8.1	Emet	39.49, 29.48	40	281	43	−94	8.80	0.11	80.00	0.51	1970 (7.1)
8.2	Demirci	39.18, 28.69	40	104	34	−90	4.70	0.16	29.38	0.19	1969 (6.1)
8.3	Bursa	40.18, 29.08	60	83	45	−90	1.69	0.23	7.35	0.05	1855 (7.4)

estimation of the macroseismic effect of the expected earthquakes in each critical region.

The estimated origin times, t_c (with uncertainty ±2.0 yr), and the magnitudes, M (with uncertainty ±0.5), for the expected main shocks are given in Table 1. The estimation of the epicentres (with uncertainty ≤120 km) was based on the best solution, as well as on the location of the corresponding faults and their probability of being activated. Based on this information the following epicentres are proposed for the corresponding regions:

Region 1, 36.5°N, 22.7°E
Region 2, 38.9°N, 23.1°E
Region 3, 38.3°N, 20.5°E
Region 4, 35.0°N, 27.4°E
Region 5, 37.4°N, 27.0°E
Region 6, 41.1°N, 20.7°E
Region 7, 40.1°N, 27.4°E
Region 8, 39.4°N, 29.4°E.

These main shocks are expected to be shallow ($h \leq 40$ km) but in regions 1 and 4 the generation of intermediate-depth earthquakes cannot be excluded.

It should be pointed out that the faults presented in this study are not in all cases identical to the faults proposed by Papazachos *et al.* (2001b). The main reason is that for several large ruptures Papazachos *et al.* (2001b) only presented the sections of the zone that are known to have ruptured (up to a certain magnitude and corresponding rupture length) from instrumental and historical information. In a few cases the faults shown in Fig. 2 are located on the same rupture zone but correspond to different sections of the zone (1.1, 2.2, 4.2) depicted by Papazachos *et al.* (2001b). Moreover, in several cases the presented faults have slightly different lengths (e.g. 1.2, 8.2, 8.3) from that depicted by Papazachos *et al.* (2001b), since the fault lengths presented in Table 2 were derived on the basis of the expected main shocks (Table 1) and the dimensions of the quiescence zone identified around each fault zone. For instance, the proposed Tenaro Fault (1.1 in Fig. 3) is part of the major thrust zone along the western Hellenic Arc, which consists of a large number of subfaults (most of which are identified in Papazachos *et al.* (2001b) which are known to have ruptured in various lengths corresponding to events up to $M_w = 8.2$. The proposed fault essentially corresponds to the section of the fault zone that is currently under a state of seismic quiescence.

It is interesting to notice that for Region 5 (southeastern Aegean) there is practically no seismic quiescence observed for any fault. This is in good agreement with the corresponding poor acceleration pattern of Fig. 2, which suggests that the acceleration identified for this region is perhaps a case of a false alarm that originated from an otherwise random space–time distribution. Furthermore, there are

two other regions (2 and 8) where all faults exhibit strong quiescence (low r_n values) for all faults. Examination of seismicity release for Region 2 presented a very stable (linear) time distribution of seismicity for the broader Ionian Islands area, showing that the quiescence pattern is only localized on all three faults, with the more prominent quiescence observed along the Lefkada Fault (Fig. 4). It should be noted that during the revision of the present paper, a strong ($M = 6.4$) main shock occurred in this fault (2003 August 14). Although the Lefkada Fault had a relatively high probability of rupturing ($P_e = 26$ per cent in Table 2) at the specified time interval, its actual magnitude is smaller that the predicted main-shock magnitude ($M = 7.0 \pm 0.5$, Table 1). Therefore, further examination of this magnitude bias is necessary before this is declared as a successful prediction.

For Region 8 (southeast Marmara) the corresponding time distribution of seismicity showed a general seismicity quiescence (for events with $M \geq 4.0$) for the broader fault area (including faults 8.1, 8.2 and 8.3), which is confirmed by the r_n values of Table 2. Examination of the space–time seismicity distribution for the broader Asia Minor area showed that this lack of seismicity in the vicinity of the faults is not a result of completeness of the catalogue. Hence it appears that the broader southeast Marmara area is going through a period of seismic quiescence, even if the broader area shows accelerated seismic energy release (Figs 1 and 2). It is very difficult to present an explanation for this spatially 'broad' quiescence area, hence new checks using updated catalogues need to be performed in the future to confirm this seismicity pattern.

DISCUSSION

The main results of the present paper are presented in two alternative forms. The first concerns the identification of eight elliptical critical regions, which are at present in accelerating seismic excitation and may lead to a main shock of a certain magnitude (see Table 1). Independently of the occurrence or not of these eight main shocks in the space, time and magnitude windows defined in the present paper, this accelerating seismic excitation is an observational fact and therefore of importance for time-dependent seismic hazard assessment, because during such excitations damaging ($M \sim 6$) earthquakes frequently occur. The results of this paper are also presented in the form of seismic faults and the corresponding probability of each fault being activated during the 5 yr from 2003–2007 (see Table 2, Fig. 3). This probability and the parameters of each fault (dimensions, orientation) allow us to estimate the parameters of strong ground motion at any site near these faults.

An important problem involved in these estimations is the determination of the uncertainties in the epicentre, time of origin and magnitude of the expected main shocks. Papazachos *et al.* (2003b) have made such estimations on the basis of results of retrospectively predicted strong main shocks ($M \geq 6.4$) in the Aegean area. We have attempted to make such estimations on the basis of the scatter of the parameter values calculated for faults in each region and by weighting each observation according to the corresponding probability, but we obtained similar results to those of Papazachos *et al.* (2003b). For this reason we have adopted in the present work an error of $\leq$120 km for the epicentre, $\pm$2.0 yr for the time of origin and $\pm$0.5 for the magnitude with a high confidence ($\sim$90 per cent). These error estimations, however, are based on the assumption that the eight main shocks predicted in the present paper will occur (with a probability of 75 per cent, since there is an additional 15 per cent chance of identification of false acceleration patterns) during the period 2003–2007 which is, of course, uncertain. Therefore reliable error analysis will have to wait until the end of this time period, when testing of the results of the present work will be possible with the use of objective data.

Whatever the percentage of success of these intermediate-term earthquake predictions, the present work will show if, at present, there is any possibility of making any significant progress in this important field of practical seismological hazard assessment and mitigation, since the patterns on which this effort has been based (accelerating seismicity, seismic quiescence) are well documented and have been widely observed by several researchers in a variety of seismotectonic regimes before strong main shocks.

ACKNOWLEDGMENTS

We would like to thank S. Hainzl and an anonymous reviewer for their reviews and valuable suggestions. The maps were made using the GMT software (Wessel & Smith 1995). Part of this research was supported by the Earthquake Protection and Planning Organization of Greece (project no 20242, Res. Com. A.U.Th.).

REFERENCES

Ben-Zion, Y., Dahmen, K., Lyakhovsky, V., Ertas, D. & Agnon, A., 1999. Self-driven mode switching of earthquake activity on a fault system, *Earth planet. Sci. Lett.,* **172,** 11–21.

Bowman, D.D., Ouillon, G., Sammis, C.G., Sornette, D. & Sornette, A., 1998. An observational test of the critical earthquake concept, *J. geophys. Res.,* **103,** 24 359–24 372.

Bufe, C.G. & Varnes, D.J., 1993. Predicting modeling of seismic cycle of the Great San Francisco Bay Region, *J. geophys. Res.,* **98,** 9871–9883.

Jaume, S.C. & Sykes, L.R., 1999. Evolving toward a critical point: a review of accelerating seismic moment/energy release prior to large and great earthquakes, *Pure appl. Geophys.,* **155,** 279–306.

Mogi, K., 1981. Seismicity in western Japan and long-term earthquake forecasting, in *Earthquake Prediction: an International Review,* Maurice Ewing Series 4, American Geophysical Union Monograph, pp. 43–52, eds Simpson, D.W. & Richards, P.G., American Geophysical Union, Washington, DC.

Papazachos, C.B., 2001. An algorithm for intermediate term earthquake prediction by the accelerating seismic deformation method, *2nd Hellenic Conference on Earthquake Engineering and Engineering Seismology, 28–30 November 2001,* pp. 107–115. Technical Chamber of Greece, Thessaloniki, Greece.

Papazachos, C.B., 2003. Minimum preshock magnitude in critical regions of accelerating seismic crustal deformation, *Boll. Geof. Teor. Appl.,* **44,** 103–113.

Papazachos, B.C. & Papazachos, C.B., 2000. Accelerating preshock deformation of broad regions in the Aegean area, *Pure appl. Geophys.,* **157,** 1663–1681.

Papazachos, C.B. & Papazachos, B.C., 2001. Precursory accelerating Benioff strain in the Aegean region, *Ann. Geofis.,* **44,** 461–474.

Papazachos, B.C. & Papazachou, C.B., 2003. *The Earthquakes of Greece,* Ziti Editions, Thessaloniki.

Papazachos, B.C., Karakaisis, G.F., Papazachos, C.B., Scordilis, E.M. & Savaidis, A.S., 2001a. A method for estimating the origin time of an ensuing mainshock by observations of preshock crustal seismic deformation, in *Proceedings of the 9th International Congress of the Geological Society of Greece, Athens, 20–25 Sept. 2001,* Vol. 4, pp. 1573–1582. Geological Society of Greece, Thessaloniki, Greece.

Papazachos, B.C., Mountrakis, D.M., Papazachos, C.B., Tranos, M.D., Karakaisis, G.F. & Savvaidis, A.S., 2001b. The faults which have caused the known major earthquakes in Greece and surrounding region between the 5th century BC and today, *Proceedings of the Second Hellenic Symposium on Earthquake Engineering and Engineering Seismology, Thessaloniki, 28–30 November 2001,* 1, 17–26. Technical Chamber of Greece, Thessaloniki, Greece.

Papazachos, C.B., Karakaisis, G.F., Savvaidis, A.S. & Papazachos, B.C., 2002a. Accelerating seismic crustal deformation in the southern Aegean area, *Bull. seism. Soc. Am.,* **92,** 570–580.

Papazachos, B.C., Savvaidis, A.S., Papazachos, C.B. & Karakaisis, G.F., 2002b. Precursory seismic crustal deformation in the area of southern Albanides, *J. Seismol.,* **6,** 237–245.

Papazachos, B.C., Savaidis, A.S., Karakaisis, G.F. & Papazachos, C.B., 2002c. Precursory accelerating seismic crustal deformation in the northwestern Anatolian fault zone, *Tectonophysics,* **347,** 217–230.

Papazachos, B.C., Comninakis, P.E., Karakaisis, G.F., Karakostas, B.G., Papaioannou, Ch.A., Papazachos, C.B. & Scordilis, E.M., 2003a. *A Catalog of Earthquakes in Greece and Surrounding Area for the Period 550 BC–2002,* Geophysics Laboratory, University of Thessaloniki.

Papazachos, C.B., Karakaisis, G.F. & Scordilis, E.M., 2003b. Results of a retrospective prediction of past strong mainshocks in the Aegean area by application of the accelerating seismic deformation method, *27th General Assembly of European Seismological Commission (ESC), Genoa, 1–6 September 2002,* p. 49.

Rundle, J.B., Klein, W., Turcotte, D.L. & Malamud, B.D., 2000. Precursory seismic activation and critical-point phenomena, *Pure appl. Geophys.,* **157,** 2165–2182.

Scholz, Ch.H., 1988. Mechanism of seismic quiescences, *Pure appl. Geophys.,* **26,** 701–718.

Sornette, A. & Sornette, D., 1990. Earthquake rupture as a critical point: consequences for telluric precursors, *Tectonophysics,* **179,** 327–334.

Sornette, D. & Sammis, C.G., 1995. Complex critical exponents from renormalization group theory of earthquakes: implications for earthquake prediction, *J. Physique I,* **5,** 607–609.

Wessel, P. & Smith, W., 1995. New version of the Generic Mapping Tools, *EOS, Trans. Am. geophys. Un.,* **76,** 329.

Wyss, M., 1986. Seismic quiescence prior to the 1983 Kaoiki ($M_s = 6.6$), Hawaii, earthquake, *Bull. seism. Soc. Am.,* **76,** 785–800.

Wyss, M., 1997. Nomination of a precursory seismic quiescence as a significant precursor, *Pure appl. Geophys.,* **126,** 320–332.

Wyss, M. & Habermann, R.E., 1988. Precursory seismic quiescence, *Pure appl. Geophys.,* **126,** 319–332.

Wyss, M., Klein, F. & Johnston, A.C., 1981. Precursors of the Kalapana $M =$ 7.2 earthquake, *J. geophys. Res.,* **86,** 3881–3900.

Yang, W., Vere-Jones, D. & Li, M., 2001. A proposed method for locating the critical point of a future earthquake using the critical earthquake concept, *J. geophys. Res.,* **106,** 4121–4128.

Zoller, G. & Hainzl, S., 2002. A systematic spatiotemporal test of the critical point hypothesis for large earthquakes, *Geophys. Res. Lett.,* **29**(11), 53–57.

Zoller, G., Hainzl, S., Kurths, J. & Zschau, J., 2002. A systematic test on precursory seismic quiescence in Armenia, *Natural Hazards,* **26,** 245–263.